

10 and 20 Gb/s all-optical RZ to NRZ modulation format and wavelength converter based on nonlinear optical loop mirror

Pavel Honzatko^{a,*}, Miroslav Karásek^{a,b}

^a*Institute of Photonics and Electronics, Academy of Sciences of the Czech Republic, v.v.i., Chaberska 57, 182 51 Prague 8, Czech Republic*

^b*CESNET, a.l.e., Žitkova 4, Prague 6, Czech Republic*

Abstract

We present experimental and theoretical results on all-optical 10 and 20 Gb/s RZ to NRZ modulation format and wavelength converter based on a nonlinear optical loop mirror (NOLM). A vector model of converter was developed and the shape of converted pulses was found analytically for particular choice of polarization states. In the experiment, non-zero dispersion shifted fiber with a length 1200m was used as a nonlinear medium. Pulses from a 10 GHz mode-locked semiconductor laser diode were modulated to form pseudorandom RZ signal and eventually time division multiplexed to 20 Gb/s. RZ pulses were subsequently converted to NRZ signal. The performance of the converter was evaluated experimentally using the data communication analyzer and bit error ratio tester.

Keywords: RZ-to-NRZ format conversion, wavelength conversion, nonlinear optical loop mirror.

1. Introduction

All optical modulation format converters become an important interface technology in optically transparent networks. Particularly, return-to-zero (RZ) to non-return-to-zero (NRZ) and NRZ/RZ converters are important for modulation format adaptation between backbone optical links and metropolitan area lines [?]. Other applications include data transmission using periodic in-line all-optical format conversion to delay the accumulation of format-specific impairments [?], and modulation format adapters at the input of measurement devices and optical receivers that are designed specifically for the NRZ signal.

*Corresponding author

Email addresses: honzatko@ufe.cz (Pavel Honzatko), karasek@ufe.cz (Miroslav Karásek)

Various RZ/NRZ converter schemes are known. Lee et al. proposed to use self-phase modulation induced spectral broadening together with group velocity dispersion in the normal regime of dispersion shifted fiber to convert 10 Gb/s RZ data signal to the NRZ format [?]. The same authors proposed to use narrowband filtration to obtain the inverted NRZ pulses from XPM signal at 10 Gb/s [?].

Number of techniques exploit the dynamics of semiconductor optical amplifiers (SOA). Interferometric schemes with Mach-Zehnder interferometer [?] at 5 Gb/s and Sagnac interferometer at 10 Gb/s [?] were tested. The later configuration is often referred to as a semiconductor laser amplifier in the loop mirror (SLALOM). The semiconductor optical amplifier is displaced from the middle of the loop by an optical path corresponding to the half of the bit period.

To avoid patterning effects, these techniques should use semiconductor devices with fast dynamics supplemented with pulse multiplier at the input. Such approach was demonstrated with an integrated Mach-Zehnder interferometer with SOA in each of the branches at 2.5 Gb/s [? ?]. Multiplication of input pulses was also used in RZ-to-NRZ converter based on FP-LD injection locked to the CW, proposed by Chow *et al.* [?].

Specially designed semiconductor structures has been developed for RZ/NRZ conversion like monostable multivibrator laser diode based on DFB laser with an integrated saturable absorber [?], two section SOA with saturable absorber in the middle [?], and monolithic integrated active Michelson interferometer [?]. Majority of these techniques rely on the dynamics of the particular type of SOA and lack clear design guidelines.

In our paper we revisited the scheme based on fiber nonlinear optical loop mirror. The scheme was proposed and experimentally tested by S. Bigo *et al.* at 10 Gb/s with. The authors developed the scalar model and came to the final conclusion that this scheme is impractical for conversion to true NRZ [?]. They also noted that actual performance of the device depended on the proper adjustment of the polarization controllers and was better than predicted by the scalar theory.

Experimentally we show that the scheme gives the pulses of the highest quality of all the published techniques. The scheme has potential for further miniaturization using the highly nonlinear fibers with non-zero dispersion.

We developed the vector model and derived the analytical solution in Section 2. Vector model is able to explain good results of this conversion scheme. Experimental results are presented in Section 3.

2. Theory

The RZ/NRZ modulation format converter is based on the nonlinear optical loop mirror (Fig. 1). The CW is coupled into the Sagnac interferometer using the 3 dB coupler. CW light is reflected by Sagnac interferometer in absence of the RZ-pulses. In presence of the RZ pulse, the destructive interference between the clockwise and counterclockwise light at the output port of the interferometer

changes to constructive as a result of nonlinear phase-shift acquired by the clockwise wave due to the cross-phase modulation (XPM) from RZ-pulse. The pulse at the output port is reshaped due to a walk-off between the CW and RZ-pulses. When the wavelength of the RZ pulses is close to the zero dispersion wavelength, the RZ-pulse does not change significantly its shape during the propagation in the Sagnac interferometer and almost rectangular pulses appear at the output port with leading and trailing edge transition times related to the width of the original RZ-pulses.

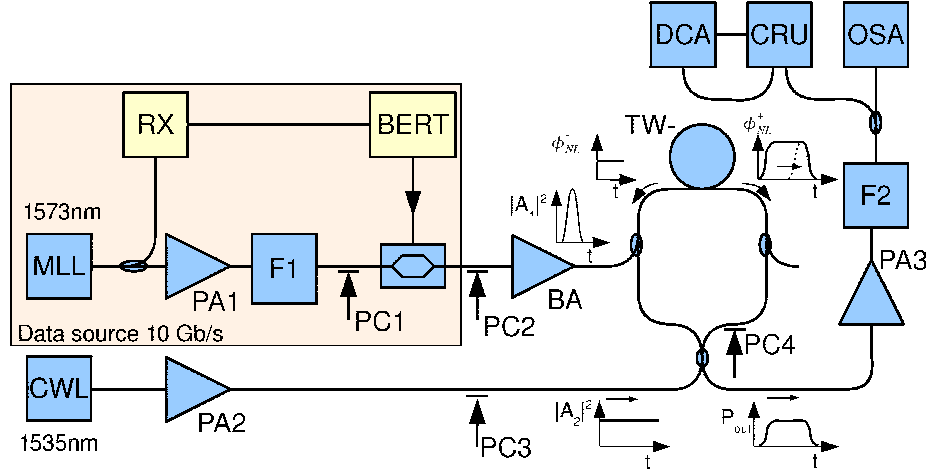


Figure 1: Experimental setup

In this section a vector model is developed and it is shown that it allows for true RZ/NRZ conversion. We will assume that generally polarized field $\mathbf{E} = xE_x + yE_y$ propagates in the isotropic optical fiber. This field induces the nonlinear polarization [?]

$$P_x = \frac{3\epsilon_0}{4}\chi_{xxxx}^{(3)} \left[\left(|E_x|^2 + \frac{2}{3}|E_y|^2 \right) E_x + \frac{1}{3}(E_x^*E_y)E_y \right], \quad (1)$$

$$P_y = \frac{3\epsilon_0}{4}\chi_{xxxx}^{(3)} \left[\left(|E_y|^2 + \frac{2}{3}|E_x|^2 \right) E_y + \frac{1}{3}(E_y^*E_x)E_x \right], \quad (2)$$

where $\chi_{xxxx}^{(3)}$ is component of third-order susceptibility tensor. We will assume that polarization components are compound of spectrally non-overlapping fields A_1 and A_2 corresponding to CW and data pulses, respectively. The resulting polarization components P_{ij} , corresponding to signals $i = 1, 2$ and polarizations $j = x, y$, have quite complicated form

$$P_{1x} = \frac{3\epsilon_0}{4}\chi_{xxxx}^{(3)} [(|A_{1x}|^2 + 2|A_{2x}|^2) A_{1x}] \quad (3)$$

$$\begin{aligned}
& + \frac{2}{3} (|A_{1y}|^2 + |A_{2y}|^2) A_{1x} + \frac{2}{3} A_{2y}^* A_{2x} A_{1y} \\
& + \frac{1}{3} (A_{1x}^* A_{1y}^2 + A_{2x}^* A_{2y} A_{1y} + A_{2x}^* A_{1y} A_{2y}) \Big], \\
P_{1y} & = \frac{3\epsilon_0}{4} \chi_{xxxx}^{(3)} [(|A_{1y}|^2 + 2|A_{2y}|^2) A_{1y} \\
& + \frac{2}{3} (|A_{1x}|^2 + |A_{2x}|^2) A_{1y} + \frac{2}{3} A_{2x}^* A_{2y} A_{1x} \\
& + \frac{1}{3} (A_{1y}^* A_{1x}^2 + A_{2y}^* A_{2x} A_{1x} + A_{2y}^* A_{1x} A_{2x}) \Big], \tag{4}
\end{aligned}$$

Similar equations can be obtained for components $P_{2x,y}$. Further analysis will be greatly simplified if we will consider a special case, when the input CW A_1 and data stream A_2 are x-polarized and polarization controller PC_4 is set in such a way that it changes x-polarization into y-polarization. Then all coherent terms leading to nonlinear polarization rotation will disappear. More over, we will assume that the power of CW is negligible with respect to power of data pulses $|A_{1x,y}|^2 \ll |A_{2x}|^2$ and we will neglect the dispersion of data pulses and of cross-phase modulated CW. General analysis is out of the scope of this paper and will be published elsewhere.

Using these assumptions, we will get for the clock-wise component of CW A_{1x}^+ , and the counter clock-wise component A_{1y}^- the following nonlinear equations

$$\begin{aligned}
\left(\partial_z + \frac{1}{v_{g1}} \partial_t \right) A_{1x}^+ & = 2i\gamma |A_{2x}|^2 A_{1x}^+, \\
\left(\partial_z + \frac{1}{v_{g1}} \partial_t \right) A_{1y}^- & = \frac{2}{3} i\gamma |A_{2x}|^2 A_{1y}^-, \tag{5}
\end{aligned}$$

where $\gamma = 6\pi\chi_{xxxx}^{(3)}/(8n\lambda A_{eff})$ is the nonlinear coefficient, n is the refractive index, A_{eff} is the effective mode area, and $v_{g1,2}$ are the group velocities. These equations have a simple analytical solutions in the reference frame in which the CW rests [?]

$$\begin{aligned}
A_{1x}^+(z, t) & = A_{1x}^+ \exp \left(2i\gamma \int_0^z |A_2(0, t + \sigma\xi)|^2 d\xi \right), \\
A_{1y}^-(z, t) & = A_{1y}^- \exp \left(\frac{2}{3} i\gamma \bar{P}_2 z \right) \tag{6}
\end{aligned}$$

where $\sigma = 1/v_{g1} - 1/v_{g2}$ is the parameter describing the walk-off per unit length, and \bar{P}_2 is the average power of data pulses in the loop.

Assume that the RZ pulses have initially a secant-hyperbolic shape with the peak power P_p and a full-width in half-maximum $T_p = 1.763\tau$,

$$A_2(0, t) = \sqrt{P_p} \operatorname{sech}[t/\tau]. \tag{7}$$

Using equations (6) and (7), we can calculate the nonlinear phase shifts acquired by the clock-wise and counter clock-wise signals in the loop of length L

$$\varphi_{NL}^+ = 2\gamma P_p \int_0^L \operatorname{sech}^2[(t + \sigma\xi)/\tau] d\xi \quad (8)$$

$$= 2\frac{\tau}{\sigma}\gamma P_p \{\tanh[(t + \sigma z)/\tau] - \tanh[t/\tau]\}.$$

$$\varphi_{NL}^- = \frac{2}{3}\gamma\bar{P}_2L. \quad (9)$$

Finally, the transmission function of Sagnac loop is

$$T = \sin^2 [(\varphi_{NL}^+ - \varphi_{NL}^-)/2]. \quad (10)$$

The peak nonlinear phase shift of the signal that co-propagates with data pulses is not explicitly dependent on the length of the fiber. It is proportional to the ratio of pulse width and walk-off per unit length, τ/σ , instead,

$$\varphi_p^+ = 4\frac{\tau}{|\sigma|}\gamma P_p. \quad (11)$$

The energy of secant-hyperbolic pulse is $E_p = 2P_p\tau$. If we take equal probabilities of "zeros" and "ones" in data stream, the average power \bar{P}_2 is related to the peak power P_p as $\bar{P}_2 = P_p\tau/T_b$. For true RZ/NRZ conversion, the wavelength separation of data signal and CW should be chosen in such a way that the walk-off between them is equal to the bit period, $\sigma L = T_b$. Using these relations in equation (11), we have

$$\varphi_p^+ = 4\gamma\bar{P}_2L. \quad (12)$$

This expression is independent of the data pulse duration. It can be explained by the fact, that for fixed pulse energy, the m -times shorter pulse have m -times higher peak power and m -times shorter interaction time due to the walk-off. When "one" is transmitted, the peak differential phase shift is

$$\delta\varphi_1 = \frac{\varphi_p^+ - \varphi_{NL}^-}{2} = \frac{5}{3}\gamma\bar{P}_2L. \quad (13)$$

For "zero" we have a nonlinear phase shift

$$\delta\varphi_0 = -\frac{\varphi_{NL}^-}{2} = -\frac{1}{3}\gamma\bar{P}_2L. \quad (14)$$

We can see that even for the case of maximum conversion efficiency $\delta\varphi_1 = \pi/2$, an extinction ratio more than 10 dB can be achieved for given selection of polarization states. This could be compared to the scalar theory [?], where $\varphi_p^+ = 4\gamma\bar{P}_2L$, $\varphi_{NL}^- = 2\gamma\bar{P}_2L$, $\delta\varphi_1 = 2\gamma\bar{P}_2L$ and $\delta\varphi_0 = -2\gamma\bar{P}_2L$. It can be seen that the scalar theory precludes correct functioning of the converter.

Practically the same results would be obtained for Gaussian pulses [?]

$$A_2(0, t) = \sqrt{P_p} \exp(-t^2/2\tau^2), \quad (15)$$

where the width-parameter τ is related to the full-width in half-maximum T_p as

$$\tau = \frac{T_p}{2\sqrt{\ln 2}}. \quad (16)$$

The nonlinear phase shift originating from the XPM can be found from equation (6) as

$$\begin{aligned} \varphi_{NL}^+ &= 2\gamma P_p \int_0^z \exp[-(t + \sigma\xi)^2/\tau^2] d\xi & (17) \\ &= \sqrt{\pi} \frac{\tau}{\sigma} \gamma P_p \{ \operatorname{erf}[(t + \sigma z)/\tau] - \operatorname{erf}[t/\tau] \}. \\ \varphi_{NL}^- &= \frac{2}{3} \gamma \bar{P}_2 L. & (18) \end{aligned}$$

The expressions for the peak nonlinear phase shifts in terms of average power are the same as for hyperbolic-secant pulses and the differential nonlinear phase shifts for marks and spaces are given by equations (13) and (14). It means that the choice of the shape of data pulses influences only the leading and trailing edge of the converted pulse. Otherwise the performance of the converter is the same regardless of the shape of input data pulses.

3. Experimental Results

The experimental setup is shown in Fig. 1. The heart of the RZ-NRZ converter is the fiber Sagnac interferometer made of 1200 m of dispersion shifted fiber (NZ-DSF, OFS TW⁻). As a source of RZ pulses we used the mode-locked laser (u^2t) generating a periodic train of pulses with repetition rate 10 GHz and pulse-width 1.5 ps. These pulses were preamplified, filtered to increase their width to 8 ps, and modulated with Mach-Zehnder intensity modulator MOD driven from the pseudorandom bit sequence generator PRBS (up to $2^{31} - 1$, Centellax), that was synchronized to the mode-locked laser signal via receiver RX and clock recovery unit CR. Pulses from the data source were amplified to 27 dBm by booster amplifier BA and coupled into the Sagnac loop using the coarse wavelength division multiplexer (CWDM) centered at 1571 nm (Opneti). At the output of the NZ-DSF, the RZ pulses and CW were separated by another CWDM. The average power of data pulses inside the loop was around 26dBm. The energy of pulses coupled into the NZ-DSF was estimated to be 80 pJ and their peak power to be 4.4 W. The nonlinear phase shift was estimated using the equation (13) as $\delta\varphi_1 \approx 1.6$ assuming the nonlinear index of NZ-DSF fiber $\gamma = 2 \text{ W}^{-1}\text{km}^{-1}$. This value of nonlinear phase-shift is close to the optimal value of $\pi/2$.

Light of a CW laser was amplified to 12 dBm and coupled into the interferometer using 3 dB-coupler. The wavelength difference between the CW and RZ-data was chosen such that the walk-off was equal to the bit period. The

group delay between the CW and RZ-pulses is given by the integral

$$\begin{aligned}
 \tau_g &= \int_{\lambda_{CW}}^{\lambda_{RZ}} D(\lambda)Ld\lambda \\
 &= \int_{\lambda_{CW}}^{\lambda_{RZ}} [S(\lambda - \lambda_0) + D_0] Ld\lambda \\
 &= \frac{S(\lambda_{RZ}^2 - \lambda_{CW}^2)L}{2} + (D_0 - S\lambda_0)(\lambda_{RZ} - \lambda_{CW})L.
 \end{aligned} \tag{19}$$

For the fiber used in the Sagnac interferometer (NZ-DSF TW⁻, OFS) we measured a value of dispersion $D_0 = -2.42$ ps/nm/km and a dispersion slope $S = 0.086$ ps/nm²/km at $\lambda_0 = 1550$ nm. In the experiment, the wavelength of the CW was 1535 nm while the source of RZ-pulses worked at the wavelength 1573 nm giving the walk-off approximately 100 ps. The dispersion of NZ-DSF at this wavelength is approximately -0.5 ps/nm/km and can be neglected because the dispersion length of RZ pulses is much longer than the length of the loop.

Polarization controllers (PC2-PC4) were used to set the optimal suppression of the CW and to obtain the best shape of converted pulses. The converted signal was amplified by the preamplifier PA and once more filtered in F2 with bandwidth of 0.9 nm. The NRZ pulses were analyzed by the data communication analyzer (DCA 8100, Agilent) and by BERT (TG1B1-A, Centellax). Both of them were synchronized from the 10 GHz clock recovery unit (83495A, Agilent). The eye diagram of input RZ pulses and of converted NRZ pulses for 10 Gb/s data stream can be seen in Fig. 2. It can be seen that an excellent quality of converted signal can be attained. As a detector for the BER measurement we used 40 Gb/s digital receiver (u^2t , DPRV2021A) that needs relatively high input power and has a higher noise figure due to the wide bandwidth compared to a standard 10 Gb/s receiver. Nevertheless, the bit error ratio of the order 10^{-12} for the input power of -6 dBm was demonstrated without any floor as can be seen in Fig. 3. Even better results could be expected for standard 10 Gb/s receiver.

We also performed an experiment with format conversion at 20 Gb/s. The signal from our RZ-pulses source was multiplexed to 20 Gb/s in an optical time domain multiplexer (U2T) preserving the PRBS 2⁷-1. The source of RZ-pulses was tuned to 1547 nm and amplified in BA to 27.5 dBm. The appropriate walk-off of 50 ps was achieved for CW tuned to 1534 nm. For a repetition rate of 20 Gb/s we were unable to synchronize the DCA to the converted pulses due to the lack of appropriate clock recovery unit. Therefore, we synchronized the DCA from the source of the pulses. For this reason, a higher jitter appears in measured eye diagrams as can be seen in Fig. 4. Nevertheless, the eye is wide opened and there is no fundamental limitation on the performance at this repetition rate. Similar jitter appears on the eye diagram even at 10 Gb/s when the DCA is synchronized in this way, deteriorating the eye diagram considerably with respect to the Fig. 2. We firmly believe that a better eye diagram with lower jitter would be measured with DCA synchronized to converted RZ pulses.

4. Conclusions

Modulation format converter based on nonlinear optical loop mirror was proposed by Bigo *et al.*. The authors developed a scalar theory and concluded that the converter is not suitable for true RZ/NRZ conversion. For proper adjustment of polarization controllers they observed better results in the experiment than those predicted by the scalar theory.

In this paper we developed the vector model of modulation format converter based on nonlinear optical loop mirror and found an analytical solution for the shape of converted NRZ pulses under the assumption of the negligible RZ pulse dispersion and for particular choice of polarization states. For these polarization states, the nonlinear polarization rotation is avoided and we predicted the extinction ratio better than 10 dB for regime with maximum conversion efficiency. The theoretically predicted results were confirmed in the experiment. We demonstrated the performance of the RZ/NRZ converter at 10 Gb/s and 20 Gb/s and we showed that this technique gives converted pulses of very high quality. Bit-error ratio better than 10^{-12} was achieved at 10 Gb/s.

Acknowledgments

This project was supported by the program “Information society” of the Czech Academy of Sciences (1ET300670502), by the Ministry of Education, Youth and Sports of the Czech Republic under project number OE08021 and partly by Research plan of CESNET, a.l.e., MSMT 6383917201.

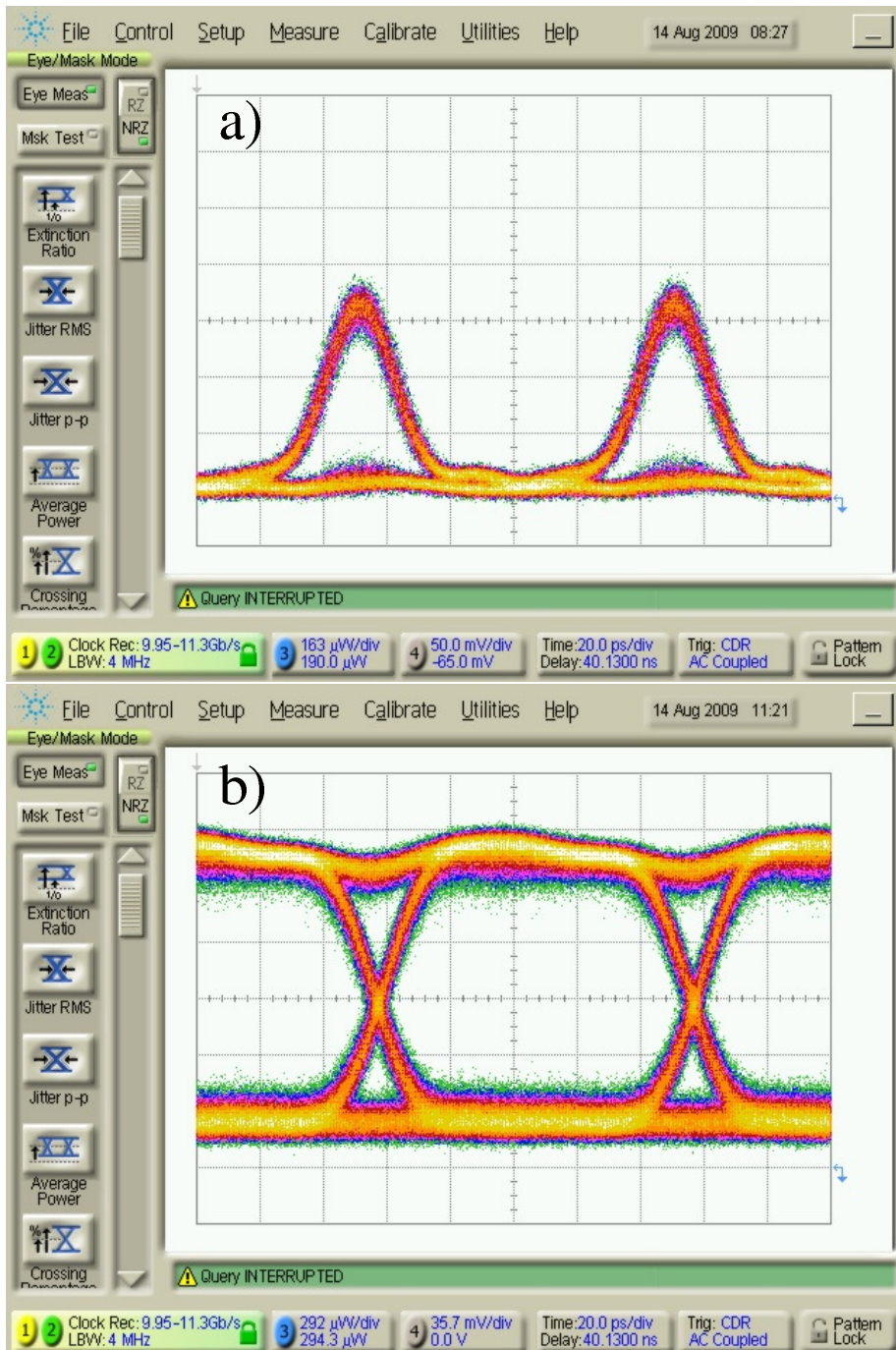


Figure 2: Eye diagram (a) of input pulses and (b) of converted NRZ pulses at 10 Gb/s.

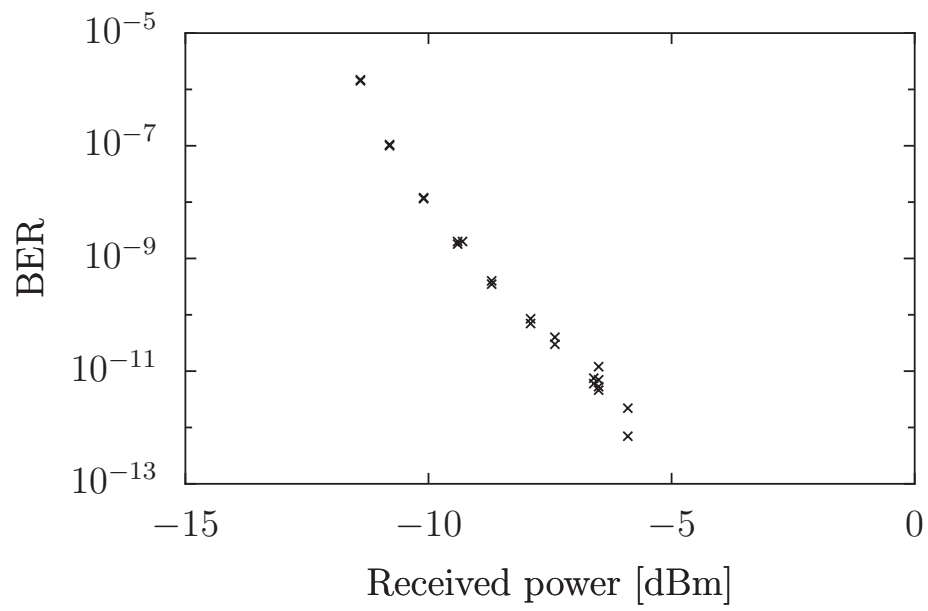


Figure 3: Bit-error ratio measurement at 10 Gb/s.

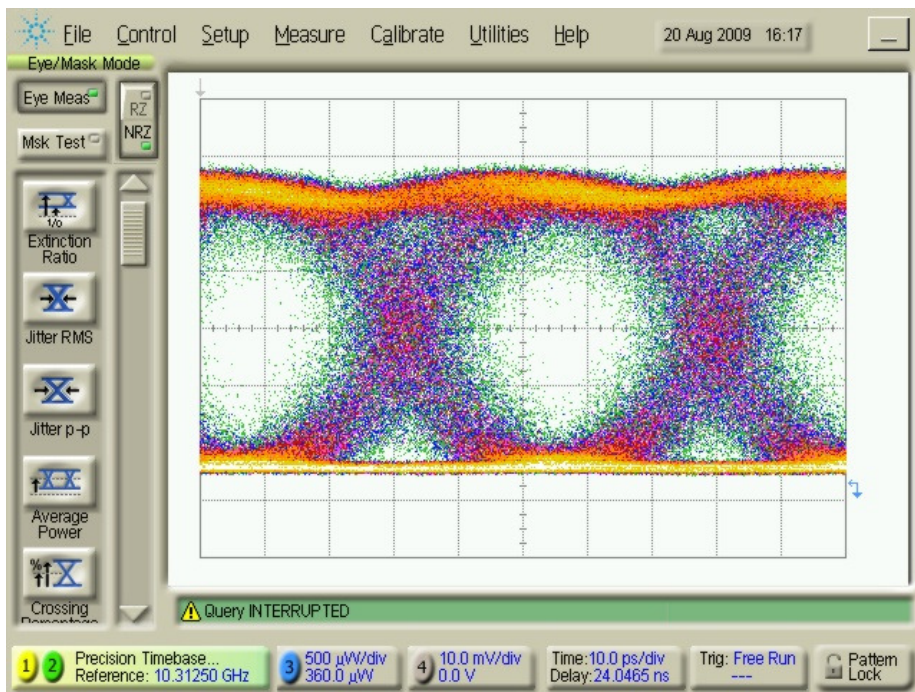


Figure 4: Eye diagram of converted NRZ pulses at 20 Gb/s.